

Observation of the Ion Resonance Instability

A. J. Peurrung, J. Notte, and J. Fajans

Department of Physics, University of California at Berkeley, Berkeley, California 94720

(Received 21 September 1992)

Observation of the ion resonance instability in a pure electron plasma trap contaminated with a small population of ions is reported. The ion population is maintained by ionization of the background gas. The instability causes the plasma to move steadily off-center while undergoing $\ell = 1$ diocotron oscillations. The observed scaling of the maximum growth point is presented, and the growth rate and its dependence on ion density are discussed. Several aspects of the observed behavior are not in agreement with previous theory but derive from the transitory nature of the ion population.

PACS numbers: 52.25.Wz, 52.35.Py, 52.35.Qz, 52.40.Mj

A pure electron plasma column, confined within a conducting cylinder by an axial magnetic field, is subject to an instability if the plasma is contaminated by a small number of oppositely charged ions. This instability, named the ion resonance instability by Levy, Daugherty, and Buneman [1], manifests itself by the gradual displacement of the plasma column from the cylinder axis. Growth takes place when the frequency of the off-axis diocotron oscillation of the electron column [2, 3] is close to the frequency of the ion oscillations through the potential well of the electron plasma. Maximum growth occurs when these frequencies are approximately equal, and growth persists even for arbitrarily small ion densities.

In this Letter we describe the first direct observations of the ion resonance instability. As predicted, the instability grows when the electron density, the plasma radius, and the applied magnetic field satisfy the frequency matching (resonance) condition. As long as the fractional neutralization of the electron column is small [4], the ion density affects the growth rate of the instability, but does not shift the position of maximum growth. Growth occurs in a broad region surrounding the resonance, and the displacement of the plasma column increases as $D \propto t$, not as $D \propto e^{\Gamma t}$. The analysis of Levy, Daugherty, and Buneman was for the case of a permanently trapped ion population. In our experiment, however, the ions are continuously created by ionization of the background neutral molecules by the energetic electrons in the plasma, and they continuously drift axially out of the plasma. Several of our observations disagree with the predictions of the trapped ion model of Levy, Daugherty, and Buneman, but agree with a new theory that accounts for the transient nature of the ion population [5].

Whether by trapped or transient ions, deliberately or inadvertently, several current and planned non-neutral plasma experiments will be partially neutralized [6–8]. For example, several planned experiments on antihydrogen production require the addition of protons to a trapped positron plasma. In toroidal geometries, the high plasma temperatures and the lack of axial ion loss

routes make the ion resonance instability an especially severe problem. Indeed, the instability has been suspected as the dominant mechanism for plasma loss in several toroidal experiments [9–11]. In general, without both extremely low background pressures and low electron temperatures, ions will always be present in any standard Penning trap.

Figure 1 shows the schematic of our trap. The electron plasma is trapped inside a series of individually biased conducting cylinders. Large negative voltages applied to the two end cylinders and a strong axial magnetic field guarantee long time confinement of the plasma [12]. When the plasma column is displaced from the center of the device, it undergoes diocotron oscillations around the device center. The instability amplitude is determined from the amplitude and frequency of the signal induced by the diocotron oscillations on an electrically isolated, azimuthal wall patch [2, 13]. This method is checked by the slower, but more direct, measurement of plasma displacement with a single-shot image of the plasma obtained using a phosphor screen and charge-coupled-device camera [14].

The basic steps in the experimental cycle are plasma formation, density selection, equilibration, and instability growth. The plasma is created in a uniform magnetic field of 500 to 2000 G. The plasma radius is varied from 0.76 to 1.31 cm by setting the cathode bias voltage during plasma formation [15]. After plasma formation,

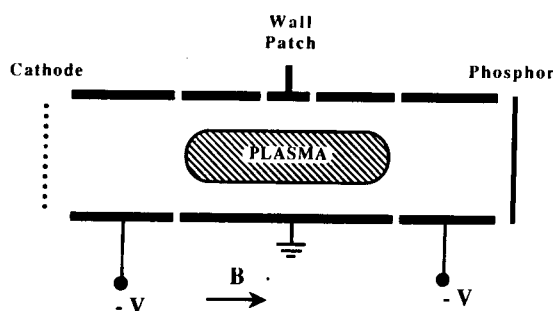


FIG. 1. Trap schematic.

we select the electron density by repeatedly splitting the plasma axially into two parts, removing the smaller part, and then expanding the larger part back to its original length. This procedure yields plasmas with accurate and repeatable densities below $5.0 \times 10^7 \text{ cm}^{-3}$. After the first several cycles, the measured [16] plasma temperature remains constant to within 12%. Next, the plasma is allowed to equilibrate, during which time active feedback from an electrically isolated wall patch [17] forces the plasma towards the device center, suppressing the ion resonance instability. After a suitable equilibration time, the feedback is terminated, allowing the instability to grow freely.

The instability results from a resonant interaction between the individual ion motion, and the bulk plasma's diocotron oscillation. Ignoring the effect of the magnetic field on the ion motion, the oscillation frequency of the ions in the bulk plasma's space charge is $\sqrt{2\pi n_e e^2 / m_i}$, where the ion mass is m_i , and the electron density is n_e . We have assumed that the plasma has a uniform radial density profile with a sharp radial edge, thereby creating a parabolic potential well with a unique ion oscillation frequency. The frequency of diocotron oscillation of the off-center plasma is $2\pi e c n_e \rho^2 / B$, where B is the magnetic field and ρ is the plasma radius scaled by the wall radius [3]. Equating these two frequencies yields the basic form of the resonance condition (valid for small plasma radii), $\rho^4 \propto B^2 / n_e$. The theory of Levy, Daugherty, and Buneman [1] gives the exact resonance condition

$$\frac{\rho^4}{1 - \rho^2} = \frac{B^2}{n_e} \left(\frac{1}{2\pi m_i c^2} \right). \quad (1)$$

The above resonance condition predicts that, at fixed plasma radius ρ , maximum growth occurs for a constant value of B^2 / n_e . To test this prediction, we measure the instability growth rate at many different values of B and n_e while holding ρ constant. We find that, although growth occurs over a wide range of densities and magnetic fields, a clearly identifiable maximum

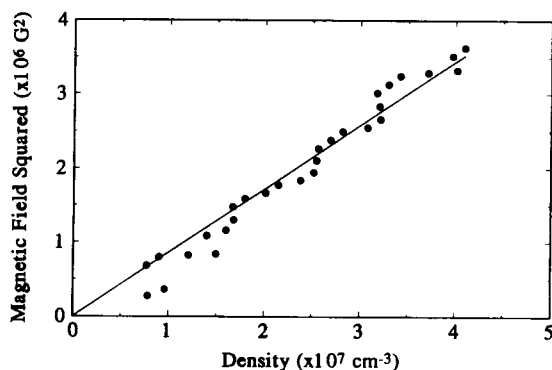


FIG. 2. Resonant points with constant radius but variable electron density and magnetic field. The data are fitted by a line of constant B^2 / n_e . The plasma radius is held at 1.15 cm, corresponding to $\rho = 0.60 \pm 0.005$.

growth "ridge" runs through the data. Figure 2 shows points which lie at the top of this ridge, along with a fitted straight line, constrained to pass through the origin, showing the prediction of the resonance condition. The actual plasma profile, as measured by the pinhole imaging technique [18], is slightly rounded and has an edge width of approximately (10-20)% of the plasma radius. The densities and radii quoted in this paper are the values which optimize the fit between the idealized square profiles and the observed rounded profiles. Consequently, there may be some systematic errors in density and radius. The low magnetic field points which deviate from the line in Fig. 2 may be affected by an increase in ion density due to rapid radial expansion heating of the plasma. Other features of the growth data also depend only on the combined parameter B^2 / n_e . For example, the width of the growth region depends only on B^2 / n_e , and the set of points where the growth rate just falls to zero lie on two lines of constant B^2 / n_e .

We test the radial dependence of Eq. (1) by finding maximum growth rate points for a variety of radii. Figure 3 shows a number of such points. The axes are chosen so that points satisfying the resonant condition fall on a straight line through the origin. The high confidence round symbols in Fig. 3 are derived from two fitted lines for resonant points of constant radius, one of which is shown in Fig. 2. The other data (shown as square points in Fig. 3) are found from a constant density scan of growth rate over the magnetic field and plasma radius. Although the plasma radius is limited in range, Eq. (1) is very sensitive to ρ because of the ρ^4 term. We use the slope of the fitted line in Fig. 3 and Eq. (1) to find that the ion mass is 48 ± 16 amu. The uncertainty comes predominantly from errors in determining the plasma radius. Although we cannot specify exactly which ion species are responsible for the resonance, this mass range includes several of the residual gases present in our vacuum system.

Ions in our experiment are created by ionization of the

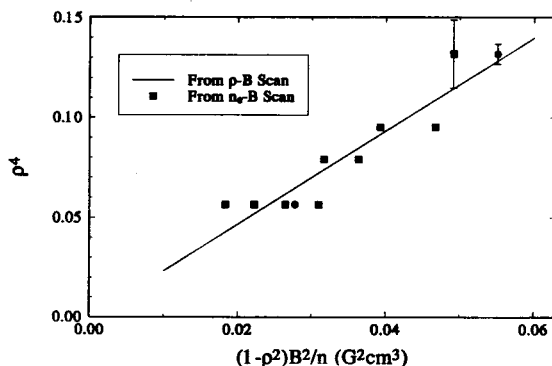


FIG. 3. Resonant points with variable radius. The axes are chosen so that if Eq. (1) describes the data, the points would fall on a straight line through the origin. The slope of the fitted line corresponds to an ion mass of 48 ± 16 amu.

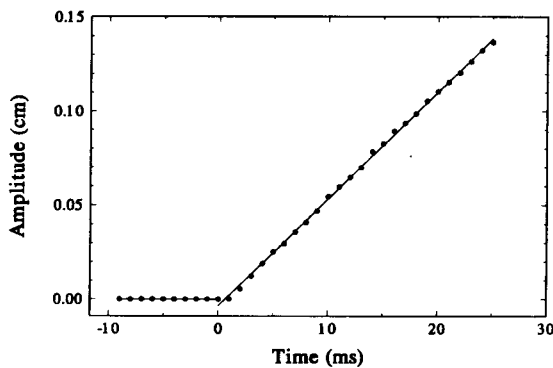


FIG. 4. Amplitude of the instability vs time. The magnetic field is 1000 G, the density is $2.75 \times 10^7 \text{ cm}^{-3}$, and the plasma radius is 1.01 cm, corresponding to $\rho = 0.53 \pm 0.005$.

background neutral gas by the energetic electrons in the plasma. Ar, H₂, H₂O, and N₂ are all present in our chamber, along with other species in lesser amounts. At our plasma temperatures ($< 8 \text{ eV}$), the small number of electrons with energy sufficient to multiply ionize a molecule and the small number of singly ionized target ions lead us to ignore the effects of ions with a charge state greater than +1. The ions retain the $\approx 300 \text{ K}$ temperature which the neutral gas acquires from the confining walls. Consequently, the ions travel at thermal velocities, and they escape axially in 0.5 ms. Since every ionization adds one electron to the plasma, the ionization rate can be determined by measuring the charge accumulation rate. Typically, the fractional neutralization is between 10^{-4} and 10^{-5} . Although ion density is most easily controlled by varying the plasma temperature, we also observe that, at constant temperature, the ionization rate increases roughly linearly with background pressure. This continuous source of new ions enables the instability to continue to grow long after the growth from this low of a static fractional neutralization would have saturated.

We observe that the instability grows slowly and algebraically. A typical growth pattern is shown in Fig. 4 for a plasma which is near a maximum growth point. The diocotron oscillation amplitude increases at a constant rate $D = gt$, taking roughly 1 s to reach the outer wall. The few observed exceptions to algebraic growth occur far from resonance and correlate with poor reproducibility. The observed resonance is also remarkably broad; Fig. 5 shows several typical growth rate scans demonstrating growth over a fourfold range in the magnetic field. These observations contradict the theory of Levy, Daugherty, and Buneman which, at low ion densities, predicts very narrow resonances and exponential growth with a rate approximately equal to the ion plasma frequency ($\approx 1 \text{ kHz}$). However, the observations agree with a new theory that takes into account the transient nature of the ion population [5].

The ion density is a strong function of the plasma temperature since only the most energetic of the plasma

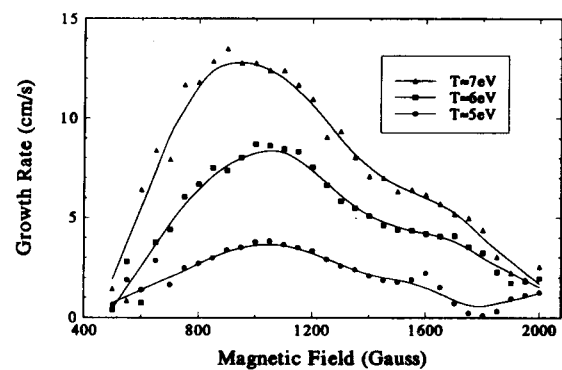


FIG. 5. Scans of the instability growth rate vs magnetic field for three different plasma temperatures T . The plasma density is $3.3 \times 10^7 \text{ cm}^{-3}$, and the radius is 0.83 cm, corresponding to $\rho = 0.44 \pm 0.005$. The growth rate is measured after a time of 14.3 ms.

electrons are able to ionize neutral molecules. For small fractional neutralization, however, the resonance condition [Eq. (1)] is independent of the ion density. Consequently, changing the plasma temperature should change the growth rate but not the resonant position. This is experimentally confirmed by Fig. 5, which shows the growth rate versus magnetic field for three different plasma temperatures. Although the growth rate changes by more than a factor of 3, there is almost no observable change in the resonant point.

Figure 6 shows the instability growth rate as a function of the ion current leaving the plasma. The ion current is measured at the end of the plasma, where the majority of ions escape and then collide with the confining wall. Levy's theory for a plasma with a resident ion population predicts that the growth rate is proportional to the square root of the ion density. Our theory for the ion resonance instability with transient ions, however, predicts that growth rate is linearly dependent on ion current. Note that there appears to be no threshold current. Large diocotron amplitudes introduce several nonlinearities

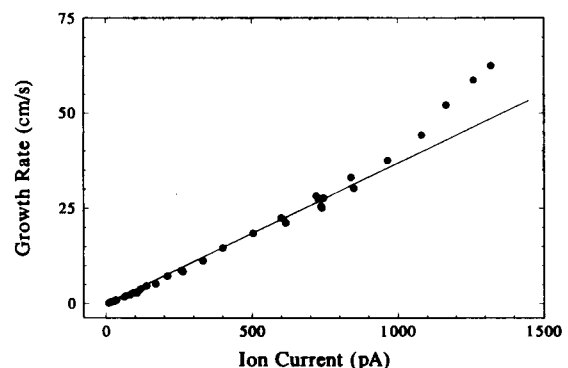


FIG. 6. Instability growth rate vs measured ion current leaving the plasma. The parameters are $B = 1000 \text{ G}$, $n_e = 6.0 \times 10^7 \text{ cm}^{-3}$, and $\rho = 0.53 \pm 0.005$. The growth rate is measured after a time of 7 ms.

ties which probably cause deviations from a straight line at high growth rates. Attempts to vary the ion density by increasing the background neutral pressure fail because the plasma temperature cannot be held constant for sufficiently long times at high pressure.

This work has been supported by the ONR and the NSF.

-
- [1] R. H. Levy, J. D. Daugherty, and O. Buneman, *Phys. Fluids* **12**, 2616 (1969).
 - [2] W. D. White, J. H. Malmberg, and C. F. Driscoll, *Phys. Rev. Lett.* **49**, 1822 (1982).
 - [3] R. H. Levy, *Phys. Fluids* **8**, 1288 (1965).
 - [4] R. C. Davidson, *Physics of Nonneutral Plasmas* (Addison-Wesley, Redwood City, 1990).
 - [5] J. Fajans (to be published).
 - [6] C. Litwin, M. C. Vella, and A. Sessler, *Nucl. Instrum. Methods Phys Res.* **198**, 189 (1982).
 - [7] A. Wolf, *Phys. Scr.* **T22**, 55 (1988).
 - [8] T. E. Cowan, R. H. Howell, and R. R. Rohatgi, *Nucl. Instrum. Methods Phys. Res., Sect. B* **56**, 599 (1991).
 - [9] J. D. Daugherty, J. E. Eninger, and G. S. Janes, *Phys. Fluids* **12**, 2677 (1969).
 - [10] W. Clark, P. Korn, A. Mondelli, and N. Rostoker, *Phys. Rev. Lett.* **37**, 592 (1976).
 - [11] P. Zaveri, P. I. John, K. Avinash, and P. K. Kaw, *Phys. Rev. Lett.* **68**, 3295 (1992).
 - [12] J. H. Malmberg and C. F. Driscoll, *Phys. Rev. Lett.* **44**, 654 (1980).
 - [13] Since we use plasmas that are long compared with the diameter of the confining cylinder, finite length effects do not affect the frequency of the diocotron oscillations.
 - [14] A. J. Peurrung and J. Fajans (to be published).
 - [15] J. H. Malmberg and J. S. deGrassie, *Phys. Rev. Lett.* **35**, 577 (1975).
 - [16] D. L. Eggleston, C. F. Driscoll, B. R. Beck, A. W. Hyatt, and T. H. Malmberg, *Phys. Fluids B* **4**, 3432 (1992).
 - [17] K. S. Fine, C. F. Driscoll, and J. H. Malmberg, *Phys. Rev. Lett.* **63**, 2232 (1989).
 - [18] C. F. Driscoll and K. S. Fine, *Phys. Fluids B* **2**, 1359 (1990).